Letters

The effect of gaseous impurities on the structure of splat-quenched nickel

In view of the recent paper by Davies and Hull [1] on the production of non-crystalline nickel by rapid quenching from the melt, it is pertinent to report some preliminary results on the effect of gaseous impurities on the stability of non-crystalline nickel produced by splat quenching. Quenching was performed in a modified "gun" [2] which normally operates in a closed inert atmosphere. Initially pure nickel (99.999%) was rapidly quenched in this apparatus in order to give a standard f c c structure for comparison with nickel–chromium austenitic steels [3, 4]. Under standard conditions, the chamber was evacuated to 10^{-5} Torr and then back filled to 500 Torr with pure argon before heating. Fig. 1 is

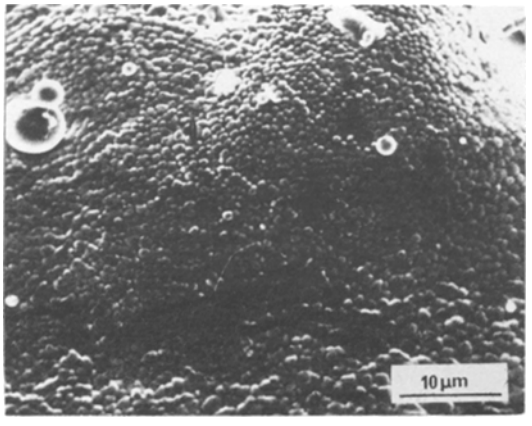

Figure 1 Scanning electron micrograph of equi-axed grain structure from the top surface of a nickel splat (p_{res} = 10^{-5} Torr).

a scanning electron micrograph of the top surface of a pure nickel splat produced in this way. A fine equi-axed grain structure is observed, and the growth direction of these grains has been perpendicular to the substrate–foil interface. In some regions (Fig. 2), dendritic structures can be observed which gives credence to the large predicted undercoolings for rapidly quenched droplets before the onset of solidification.

Transmission electron microscopy of unthinned regions of splats show random dislocation networks

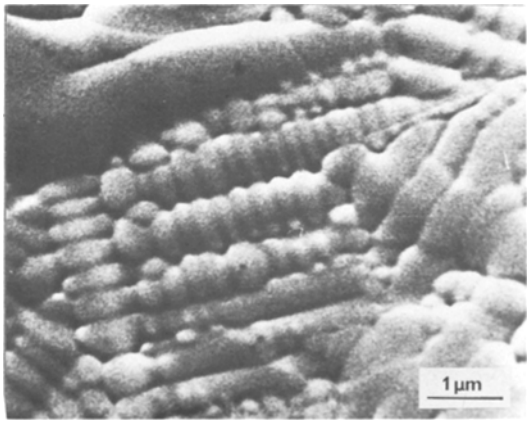

Figure 2 Thermal dendrites in splat quenched pure nickel (scanning electron micrograph).

(Fig. 3a), low-angle boundaries (Fig. 3b), and intrinsic stacking faults (Fig. 3c). There is no evidence of intrinsic dislocation loop formation as found in pure aluminium [5] or in austenitic stainless steels [3]. In very thin areas, characterized by grains lying in the foil plane [6], the grains are virtually defect-free with occasional microtwinning in some regions.

After the initial report of non-crystalline nickel produced by splat-quenching [7], we decided to investigate what role air played in the stability of this phase. Residual air pressures (p_{res}) ranging from 5×10^{-5} to 100 Torr were introduced prior to backfilling the splat quenching enclosure with pure argon. These numbers have no quantitative meaning for two reasons, (1) the argon used contains significant gaseous impurities, and (2) the graphite susceptor employed to heat the specimen getters a proportion of the residual oxygen left in the system. However, this technique did allow a qualitative assessment of the degree of impurity level.

X-ray diffraction from powdered samples was performed in a Debye–Scherrer camera with Straumanis mounting. In the main, copper $K\alpha$ was used, but $K\beta$ was also used to provide additional information for crystal structure determination. The f c c lattice parameter from the as-received annealed powder was 3.5245 Å. Fig. 4 is a plot of apparent lattice parameter against the logarithm of the par-

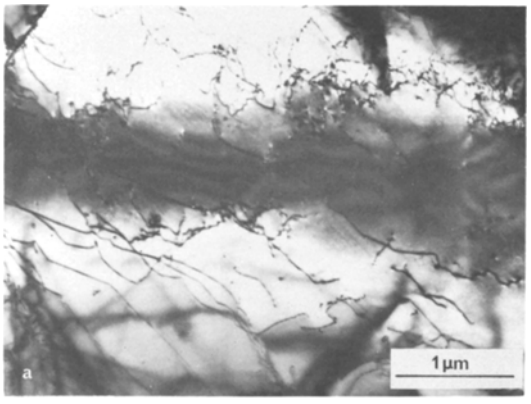

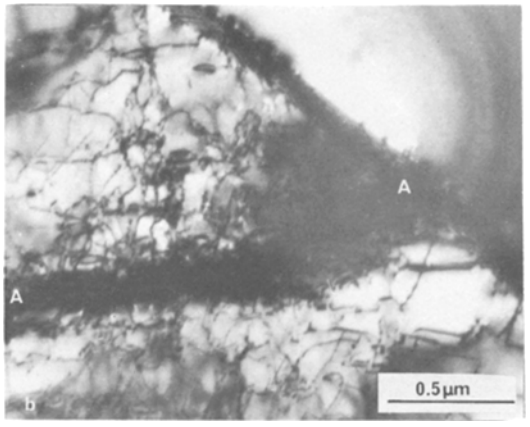

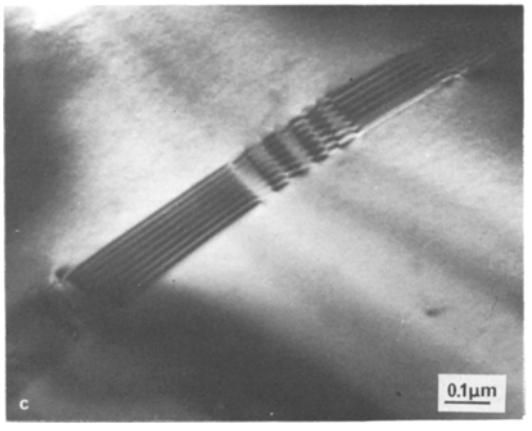

Figure 3 Transmission electron micrographs of unthinned splats at $p_{res} = 10^{-5}$ Torr. (a) Random dislocation networks; (b) low-angle boundaries (designated by line A–A); (c) intrinsic stacking faults.

tial pressure of oxygen prior to splatting. The dotted line represents the annealed powder specimen value, and the hatched region is the reasonable error band in which the lattice parameters of f c c splats would be expected to lie. Below $\log p_{O_2} = 1$, the diffraction lines become diffuse and mean lattice parameters are plotted which are significantly outside the reasonable error limits.

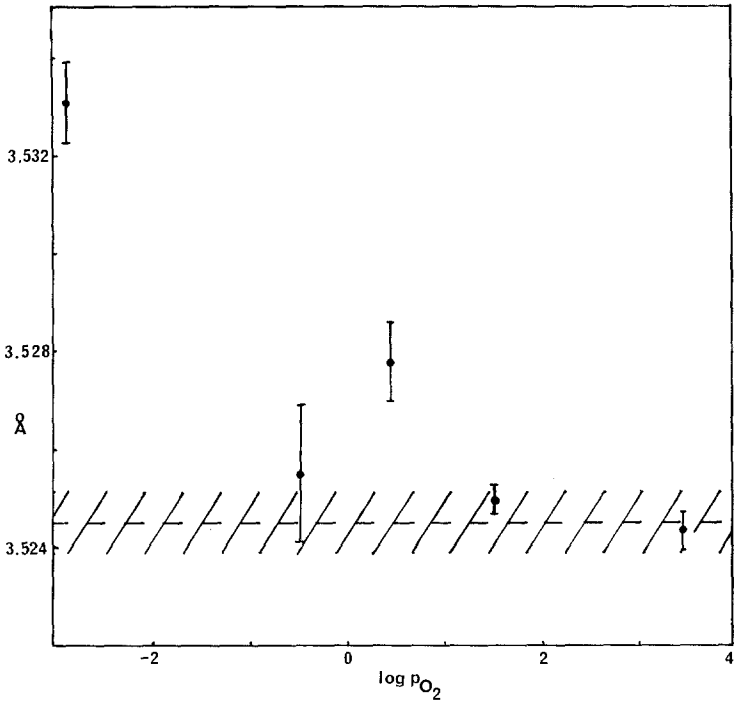

Figure 4 Apparent lattice parameter of splat-quenched nickel against the logarithm of the partial pressure of oxygen in the air admitted into the chamber prior to quenching. Dotted line represents the value of annealed nickel powder, and the appropriate error band is outlined by hatching.

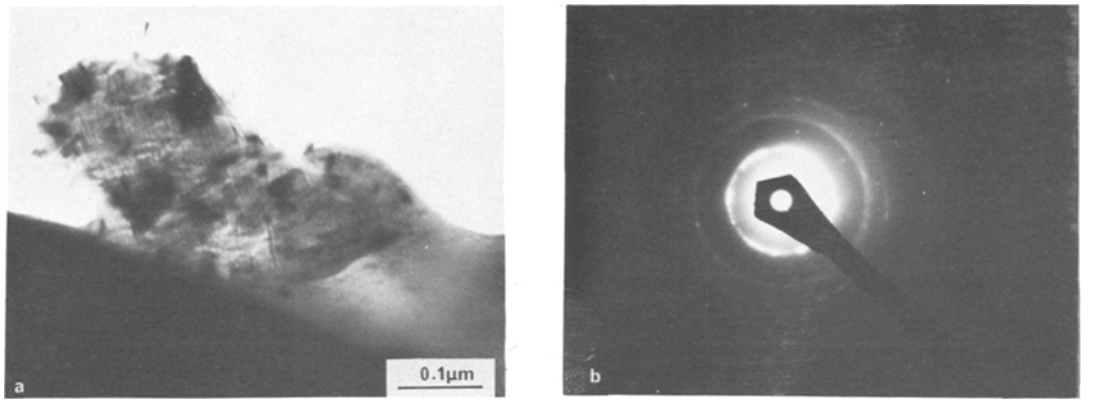

Figure 5 Transmission electron micrographs for $p_{res} = 10^{-2}$ Torr. (a) Bright-field image; (b) electron diffraction pattern from (a) indicating oxide formation.

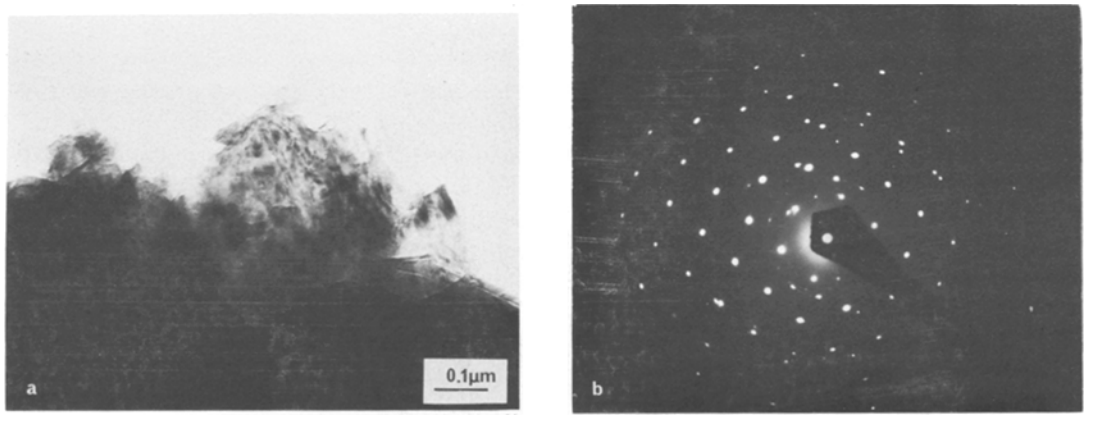

Figure 6 (a) and (b) As in Fig. 5, but $p_{res} = 100$ Torr.

Diffractometer traces from foils showed splitting of peaks in specimens quenched below log $p_{O_2} = 1$, becoming considerable in the sample produced under the lowest value of $p_{res}(5 \times 10^{-5}$ Torr). Using higher resolution X-ray techniques it can be shown that there is a two phase structure comprising of an f c c and an orthorhombic contribution. The f c c phase has a lattice parameter that lies within the error bands in Fig. 4, and tentative orthorhombic constants have been ascribed to the second phase: $a = 3.53$, $b = 3.55$, and $c = 3.57$ Å. At present a computer simulation study is in progress to determine more exact parameters for this structure. In foils produced at $p_{res} = 100$ Torr there is a low intensity diffuse diffractometer peak just before the nickel {1 1 1} peak ($42.78 \leqslant 2\theta \leqslant 43.57$) which could either be produced from the {1 1 1} nickel oxide reflection or the first diffuse ring of noncrystalline nickel [1].

Electron microscopy of foils produced in the purest atmosphere has already been described above. The main area of investigation in foils produced after the introduction of air was in regions on the edges of foils where non-crystalline nickel was apparently more easy to find [7]. Microscopy was performed in a JEOL "Jem 200A" operating at 200 kV. At $p_{res} = 10^{-2}$ Torr, small transparent regions emanated from the edges and give rise to ring diffraction patterns (Fig. 5a and b), and can be attributed to a microcrystalline oxide. Thin areas of oxide on foils produced at $p_{res} = 100$ Torr normally give a single crystal diffraction pattern on using

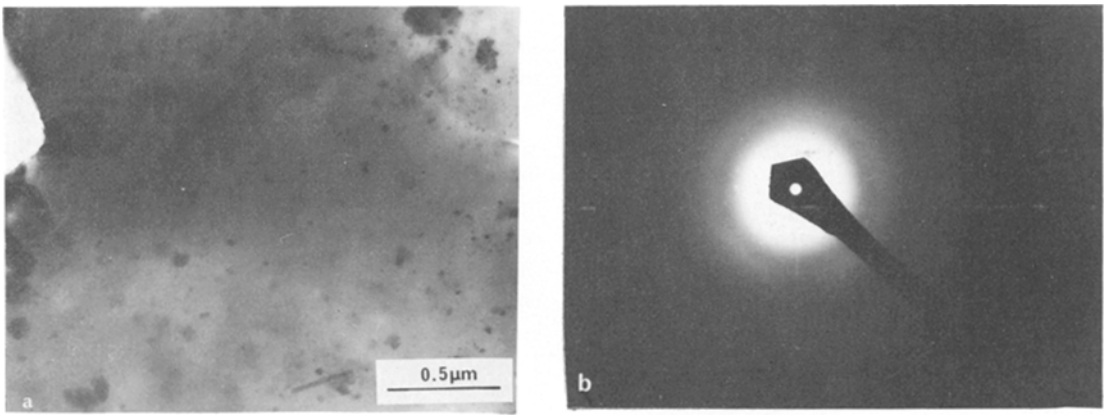

Figure 7 $p_{res} = 10^{-1}$ Torr. (a) Bright-field of non-crystalline region; (b) diffraction pattern from (a).

the smallest diffraction aperture (Fig. 6a and b). However, above $p_{res} = 10^{-1}$ Torr, it is possible to find areas which give rise to diffuse ring patterns identical with those reported by Davies and Hull [1]. Fig. 7a and b shows a bright-field micrograph and diffraction pattern from one such area.

Leung and Wright [8] have discussed the effects of impure gaseous environments on the stability of evaporated nickel films. They note that it is not possible to prepare amorphous nickel in very high vacuums ($< 10^{-6}$ Torr) and conclude that it is unlikely to be oxygen stabilized because of the dissimilarity between the interference function for amorphous nickel and other amorphous transition metals produced in the same way. However, the present results demonstrate that the amount of residual air does influence the stability of the non-crystalline form of nickel.

Acknowledgements

This work was undertaken as a Part II undergraduate project in 1974 and we would like to thank Professor R.W.K. Honeycombe for the provision of laboratory facilities. One of us (KNA) would like to acknowledge financial support from the London Borough of Barnet, whilst the other (JVW) is indebted to Foseco International for a Post-doctoral fellowship.

References

1. H. A. DAVIES and J. B. HULL, *J. Mater. Sci.* **11** (1976) 215.
2. J. V. WOOD and I. R. SARE, 2nd International Conference on Rapidly Quenched Metals, M.I.T., Boston, USA (1975).
3. J. V. WOOD and R. W. K. HONEYCOMBE, *J. Mater. Sci.* 9 (1974) 1183.
4. J. V. WOOD, Ph.D. dissertation, University of Cambridge (1974).
5. G. THOMAS and R. H. WILLENS, *Acta Met.* **12** (1964) 191.
6. J. V. WOOD and I. R. SARE, *Met. Trans.* **6A** (1975) 2153.
7. H. A. DAVIES, J. AUCOTE and J. B. HULL, *Nature (Phy. Sci.)*, **216** (1973) 13.
8. P. K. LEUNG and J. G. WRIGHT, *Phil. Mag.* **30** (1974) 995.

Received 11 February
and accepted 2 March 1976

J. V. WOOD
K. N. AKHURST
Department of Metallurgy and Materials Science,
University of Cambridge,
Pembroke Street,
Cambridge,
UK